



Research article

Analysis of the magnetohydrodynamic flow in a porous medium

E. Arul Vijayalakshmi¹, S. S. Santra², T. Botmart^{3,*}, H. Alotaibi⁴, G. B. Loganathan⁵,
M. Kannan¹, J. Visuvasam⁶ and V. Govindan⁷

¹ Department of Mathematics, Government Arts College, Ariyalur, Affiliated to Bharathidhasan University, Thiruchirappalli, Tamil Nadu, India

² Department of Mathematics, JIS College of Engineering, Kalyani, West Bengal-741235, India

³ Department of Mathematics, Faculty of Science, Khon Kaen University, Khon Kaen 40002, Thailand

⁴ Department of Mathematics and Statistics, College of Science, Taif University, P.O.Box 11099, Taif 21944, Saudi Arabia

⁵ Department of Mechatronics Engineering, Tishk International University, Erbil, KRG, Iraq

⁶ Department of Mathematics, Rathavel Subramaniam College of Arts and Science, Sullur, Coimbatore-641402, Tamil Nadu, India

⁷ Department of Mathematics, Dmi St John The Baptist University, Mangochi, Central Africa, Malawi-409

* **Correspondence:** Email: thongbo@kku.ac.th.

Abstract: This paper develops the combined effects of free convection magnetohydrodynamic (MHD) flow past a vertical plate embedded in a porous medium. The dimensionless coupled non-linear equations are solved to get the approximate analytical expression for the concentration by using the homotopy perturbation method. For all possible values of parameters, skin lubrication, Nusselt number and Sherwood number are derived.

Keywords: magnetohydrodynamic (MHD); non-linear differential equations; vertical plate; porous medium; homotopy perturbation method

Mathematics Subject Classification: 76W05, 76S05

1. Introduction

The study on flow of fluids which are electrically conducting is known as magnetohydrodynamics (MHD). The magnetohydrodynamics have important applications in the polymer industry and engineering fields (Garnier [1]). Heat transfer caused by hydromagnetism was discussed by

Chakrabarthy and Gupta [2]. Using an exponentially shrinking sheet, Nadeem et al. [3] investigated the MHD flow of a Casson fluid. Krishnendu Bhattacharyya [4] examined the effect of thermal radiation on MHD stagnation-point Flow over a Stretching Sheet.

Mixed convection magnetohydrodynamics flow is described by Ishak on a vertical and on a linearly stretching sheet [5–7]. Hayat et al. [10] examine a mixed convection flow within a stretched sheet of Casson nanofluid. Subhas Abel and Monayya Mareppa, examine magnetohydrodynamics flow on a vertical plate [11]. Shen et al. [12], examined a vertical stretching sheet which was non-linear. Ishikin Abu Bakar [13] investigates how boundary layer flow is affected by slip and convective boundary conditions over a stretching sheet. A vertical plate oscillates with the influence of slip on a free convection flow of a Casson fluid [14].

Nasir Uddin et al. [15] used a Runge-Kutta sixth-order integration method. Barik et al. [16] implicit finite distinction methodology of Crank Sir Harold George Nicolson sort Raman and Kumar [17] utilized an exact finite distinction theme of DuFort–Frankel. Mondal et al. [18] used a numerical theme over the whole vary of physical parameters. With the laplace transform method, we can determine the magnetohydrodynamic flow of a viscous fluid [19]. Thamizh Suganya et al. [20] obtained that the MHD for the free convective flow of fluid is based on coupled non-linear differential equations. In this study, the analytical approximation of concentration profiles in velocity, temperature and concentration using homotopy perturbation method (HPM).

2. Mathematical construction of the problem

The governing differential equations in dimensionless form [19] as follows:

$$\frac{d^2u}{dy^2} - Hu + Gr\theta + Gm\phi = 0, \quad (2.1)$$

$$\frac{1}{F} \frac{d^2\theta}{dy^2} = 0, \quad (2.2)$$

$$\frac{1}{Sc} \frac{d^2\phi}{dy^2} - Sr \frac{\partial^2\phi}{\partial y^2} - \gamma\phi = 0. \quad (2.3)$$

The dimensionless boundary conditions given by:

$$u = 0, \theta = 1, \phi = 0 \text{ at } y = 0 \quad (2.4)$$

and

$$u = 0, \theta = 0, \phi = 0 \text{ at } y \rightarrow \infty. \quad (2.5)$$

3. Solutions of steady-state concentration profile using the Homotopy Perturbation Method

He [21, 22] established the homotopy perturbation method, which waives the requirement of small parameters. Many researchers have used HPM to obtain approximate analytical solutions for many non-linear engineering dynamical systems [23, 24]. The basic concept of the HPM as follows:

$$\frac{d^2u}{dy^2} - Hu + Gr\theta + Gm\phi = 0 \quad (3.1)$$

$$\frac{1}{F} \frac{d^2\theta}{dy^2} = 0 \quad (3.2)$$

$$\frac{1}{Sc} \frac{d^2\phi}{dy^2} - Sr \frac{\partial^2\phi}{\partial y^2} - \gamma\phi = 0 \quad (3.3)$$

with initial and boundary conditions given by:

$$\begin{aligned} y = 0 \text{ at } u = 0, \theta = 1, C = 1 \\ y \rightarrow \infty \text{ as } u = 0, \theta = 1, \phi = 0. \end{aligned} \quad (3.4)$$

Homotopy for the above Eqs (3.1) to (3.4) can be constructed as follows:

$$(1-p) \left[\frac{d^2u}{dy^2} - Hu + Gr\theta + Gm\phi \right] + p \left[\frac{d^2u}{dy^2} - Hu + Gr\theta + Gm\phi \right] = 0 \quad (3.5)$$

$$(1-p) \left[\frac{1}{F} \frac{d^2\theta}{dy^2} - \theta \right] + p \left[\frac{1}{F} \frac{d^2\theta}{dy^2} - \theta + \theta \right] = 0 \quad (3.6)$$

$$(1-p) \left[\frac{1}{Sc} \frac{d^2\phi}{dy^2} - \gamma\phi \right] + p \left[\frac{1}{Sc} \frac{d^2\phi}{dy^2} - Sr \frac{\partial^2\phi}{\partial y^2} - \gamma\phi \right] = 0 \quad (3.7)$$

The approximate solution of the Eqs (3.5) to (3.7) are

$$u = u_0 + pu_1 + p^2u_2 + p^3u_3 + \dots \quad (3.8)$$

$$\theta = \theta_0 + p\theta_1 + p^2\theta_2 + p^3\theta_3 + \dots \quad (3.9)$$

$$\phi = \phi_0 + p\phi_1 + p^2\phi_2 + p^3\phi_3 + \dots \quad (3.10)$$

Substitution Eqs (3.5) to (3.7) in Eqs (3.8) to (3.10) respectively. We obtain the following equations

$$\begin{aligned} (1-p) \left[\frac{d^2(u_0 + pu_1 + p^2u_2 + p^3u_3 + \dots)}{dy^2} - H(u_0 + pu_1 + p^2u_2 + p^3u_3 + \dots) \right. \\ \left. + Gr(\theta_0 + p\theta_1 + p^2\theta_2 + p^3\theta_3 + \dots) + Gm(\phi_0 + p\phi_1 + p^2\phi_2 + p^3\phi_3 + \dots) \right] \\ + p \left[\frac{d^2(u_0 + pu_1 + p^2u_2 + p^3u_3 + \dots)}{dy^2} - H(u_0 + pu_1 + p^2u_2 + p^3u_3 + \dots) \right. \\ \left. + Gr(\theta_0 + p\theta_1 + p^2\theta_2 + p^3\theta_3 + \dots) + Gm(\phi_0 + p\phi_1 + p^2\phi_2 + p^3\phi_3 + \dots) \right] = 0 \end{aligned} \quad (3.11)$$

and

$$\begin{aligned} (1-p) \left[\frac{1}{F} \frac{d^2(\theta_0 + p\theta_1 + p^2\theta_2 + p^3\theta_3 + \dots)}{dy^2} - (\theta_0 + p\theta_1 + p^2\theta_2 + p^3\theta_3 + \dots) \right] \\ + p \left[\frac{1}{F} \frac{d^2(\theta_0 + p\theta_1 + p^2\theta_2 + p^3\theta_3 + \dots)}{dy^2} - (\theta_0 + p\theta_1 + p^2\theta_2 + p^3\theta_3 + \dots) \right. \\ \left. + (\theta_0 + p\theta_1 + p^2\theta_2 + p^3\theta_3 + \dots) \right] = 0, \end{aligned} \quad (3.12)$$

and

$$(1-p) \left[\frac{1}{Sc} \frac{d^2(\phi_0 + p\phi_1 + p^2\phi_2 + p^3\phi_3 + \dots)}{dy^2} - \gamma(\phi_0 + p\phi_1 + p^2\phi_2 + p^3\phi_3 + \dots) \right]$$

$$+ p \left[\frac{1}{Sc} \frac{d^2(\phi_0 + p\phi_1 + p^2\phi_2 + p^3\phi_3 + \dots)}{dy^2} - Sr \frac{\partial^2(\theta_0 + p\theta_1 + p^2\theta_2 + p^3\theta_3 + \dots)}{\partial y^2} - \gamma(\phi_0 + p\phi_1 + p^2\phi_2 + p^3\phi_3 + \dots) \right] = 0. \quad (3.13)$$

Equating the coefficient of p on both sides, we get the following equations

$$P^0 : \frac{d^2 u_0}{dy^2} - H u_0 + Gr \theta_0 + Gm \phi_0 = 0; \quad (3.14)$$

$$p^0 : \frac{1}{F} \frac{d^2 \theta_0}{dy^2} - \theta_0 = 0; \quad (3.15)$$

$$P^1 : \frac{1}{F} \frac{d^2 \theta_0}{dy^2} - \theta_0 + \theta_1 = 0; \quad (3.16)$$

$$P^1 : \frac{1}{Sc} \frac{d^2 \phi_0}{dy^2} - \gamma \phi_0 = 0; \quad (3.17)$$

$$P^1 : \frac{1}{Sc} \frac{d^2 \phi_0}{dy^2} - Sr \frac{\partial^2 \theta_0}{\partial y^2} - \gamma \phi_0 = 0. \quad (3.18)$$

The boundary conditions are

$$\begin{aligned} u_0 = 0, \theta_0 = 1, \phi_0 = 1 \text{ at } y = 0 \\ u_0 = 0, \theta_0 = 1, \phi_0 = 1 \text{ at } y \rightarrow \infty. \end{aligned} \quad (3.19)$$

and

$$\begin{aligned} u_1 = 0, \theta_1 = 0, \phi_1 = 0 \text{ at } y = 0 \\ u_1 = 0, \theta_1 = 0, \phi_1 = 0 \text{ at } y \rightarrow \infty. \end{aligned} \quad (3.20)$$

Solving the Eqs (3.9)–(3.14), we obtain

$$u_0(t) = \frac{Gr}{\sqrt{\frac{1}{F} + H}} \left[e^{-y\sqrt{\frac{1}{F}}} - e^{-y\sqrt{H}} \right] + \frac{Gm}{\sqrt{\gamma Sc + H}} \left[e^{-y\sqrt{\gamma Sc}} - e^{-y\sqrt{H}} \right]; \quad (3.21)$$

$$\theta_0(y) = e^{-y\sqrt{\frac{1}{F}}}; \quad (3.22)$$

$$\phi_0(y) = e^{-y\sqrt{\gamma Sc}}; \quad (3.23)$$

$$\phi_1(y) = \frac{ScSr}{\sqrt{F} + F\gamma Sc} \left[e^{-y\sqrt{\frac{1}{F}}} - e^{-y\sqrt{\gamma Sc}} \right]. \quad (3.24)$$

Considering the iteration, we get,

$$u(t) = \frac{Gr}{\sqrt{\frac{1}{F} + H}} \left[e^{-y\sqrt{\frac{1}{F}}} - e^{-y\sqrt{H}} \right] + \frac{Gm}{\sqrt{\gamma Sc + H}} \left[e^{-y\sqrt{\gamma Sc}} - e^{-y\sqrt{H}} \right]; \quad (3.25)$$

$$\theta(y) = e^{-y\sqrt{\frac{1}{F}}}; \quad (3.26)$$

$$\phi(y) = e^{-y\sqrt{\gamma Sc}} + \frac{ScSr}{\sqrt{F} + F\gamma Sc} \left[e^{-y\sqrt{\frac{1}{F}}} - e^{-y\sqrt{\gamma Sc}} \right]. \quad (3.27)$$

4. Approximate analytical solutions for the skin friction, Nusselt and Sherwood numbers

From the Eqs (3.25)–(3.27), we obtain

$$C_f = -\left(\frac{\partial u}{\partial y}\right)_{y=0} = \frac{\left(Gm \sqrt{\gamma Sc} - Gm \sqrt{H} + Gr(\gamma Sc + H) \sqrt{1 + \frac{R}{Pr}} + GmH \sqrt{\gamma Sc} + (-Gm - Gr)H^{\frac{3}{2}} - \gamma Gr \sqrt{HSc}\right)}{\left(\sqrt{1 + \frac{R}{Pr}} + H(\gamma Sc + H)\right)}; \quad (4.1)$$

$$N_u = -\left(\frac{\partial \theta}{\partial y}\right)_{y=0} = \sqrt{\frac{1+R}{Pr}}; \quad (4.2)$$

$$S_h = -\left(\frac{\partial \phi}{\partial y}\right)_{y=0} = \frac{ScSr(1+R) \sqrt{1 + \frac{R}{Pr}} - \sqrt{\gamma Sc} \left((-R-1) \sqrt{1 + \frac{R}{Pr}} + ((1+R)Sc - Pr\gamma)Sc\right)}{(1+R) \sqrt{1 + \frac{R}{Pr}} Pr\gamma Sc} \quad (4.3)$$

5. Results and discussion

The combined impacts of transient MHD free convective flows of an incompressible viscous fluid through a vertical plate moving with uniform motion and immersed in a porous media are examined using an exact approach. The approximate analytical expressions for the velocity u , temperature θ , and concentration profile ϕ are solved by using the homotopy perturbation method for fixed values of parameters is graphically presented.

Velocity takes time at first, and for high values of y , it takes longer, and the velocity approaches zero as time increases. The velocity of fluid rises with Gr increasing, as exposed in Figure 1.

The variations of parameter Gm are depicted in Figure 2. It has been established that as the value of increases, neither does the concentration. Gm . This is because increasing the number of ‘ Gm ’ diminishes the slog energy, allow the fluid to transfer very rapidly. The dimensionless Prandtl number is a number which combines the viscosity of a fluid with its thermal conductivity. For example, Figure 3 shows how a decrease in ‘ Pr ’ increases the concentration of velocity profile.

The Figure 4 shows how a decrease in concentration occurs when the value of H increases. As shown in Figure 5, when the Schmidt number Sc increases, the concentration of velocity profiles decreases, while the opposite is true for the Soret number Sr , as shown in Figures 6, 7 and 8, represented the radiation parameter R , chemical reaction parameter γ is increasing when it implies a decrease in concentration.

Based on Figure 9, it is evident that the thickness of the momentum boundary layer increases for fluids with $Pr < 1$. When $Pr < 0.015$, the heat diffuses rapidly in comparison to the velocity.

Figure 10 depicts the impact of the radiation parameter R on temperature profiles. The temperature profiles θ , which are a decreasing function of R , are found to decrease the flow and lower fluid velocity. As the radiation parameter R is increased, the fluid thickens, temperatures and thermal boundary layer thickness to decrease.

This statement is justified because the thermal conductivity of a fluid declines by the growing Prandtl number Pr and hence the thickness of thermal boundary layers and temperature profiles decrease as well. Based on Figure 9, we see an increase in fluid concentration with large Prandtl

numbers Pr . Radiation parameter R and temperature profiles are illustrated in Figure 10. The temperature profiles θ , which are a decreasing function of R , are initiate to reduction the flow and decline the fluid velocity. Radiation parameter R increases as fluid thickness increases, temperature increases, and thickness of thermal boundary layer decreases.

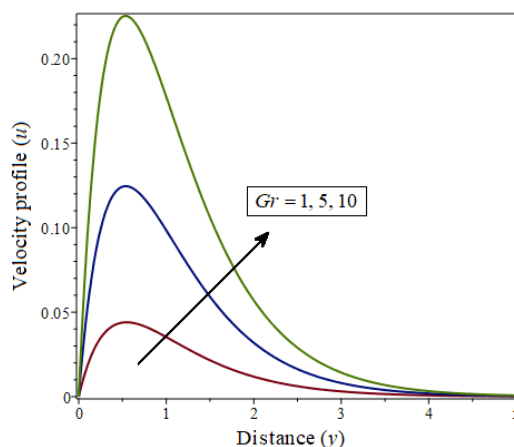


Figure 1. An illustration of velocity profiles for different values of Gr .

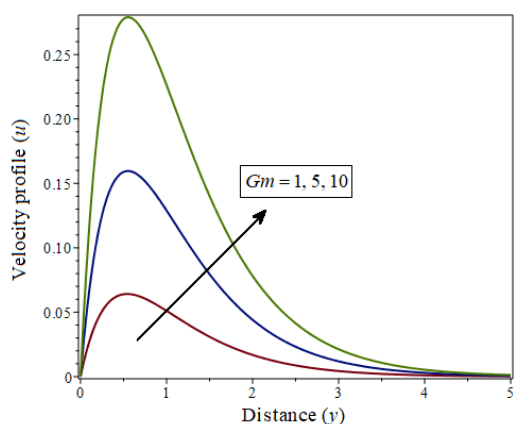


Figure 2. An illustration of velocity profiles for different values of Gm .

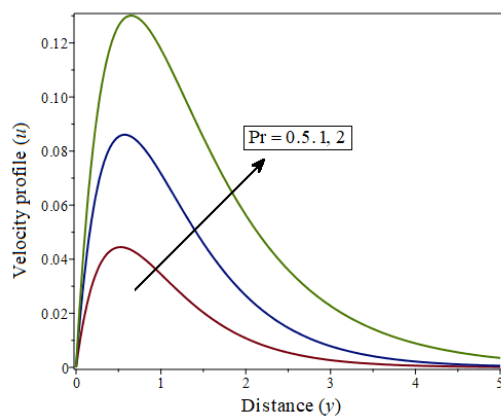


Figure 3. An illustration of velocity profiles for different values of Pr.

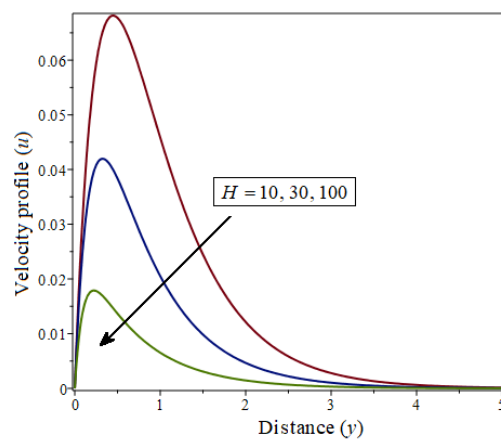


Figure 4. An illustration of velocity profiles for different values of H.

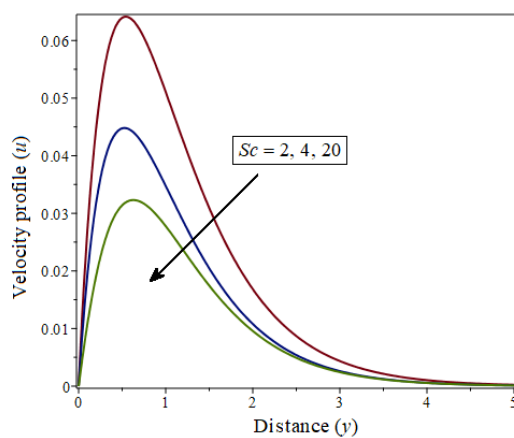


Figure 5. An illustration of velocity profiles for different values of Sc.

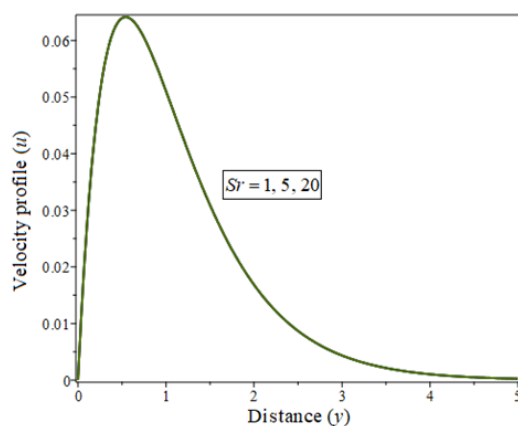


Figure 6. An illustration of velocity profiles for different values of Sr .

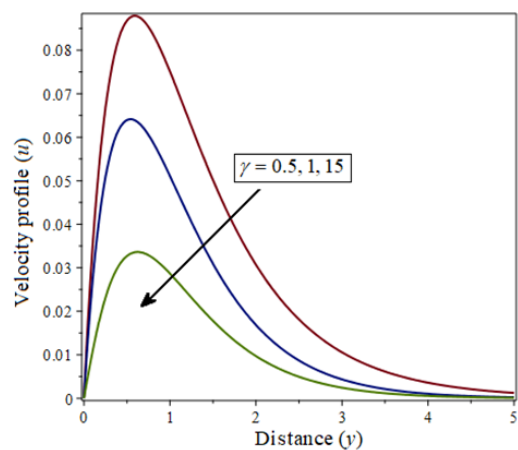


Figure 7. An illustration of velocity profiles for different values of γ .

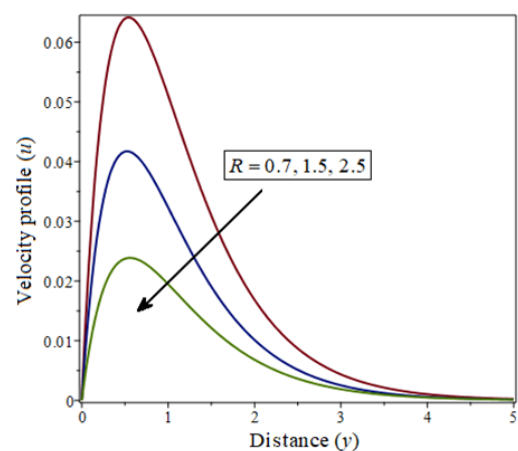


Figure 8. An illustration of velocity profiles for different values of R .

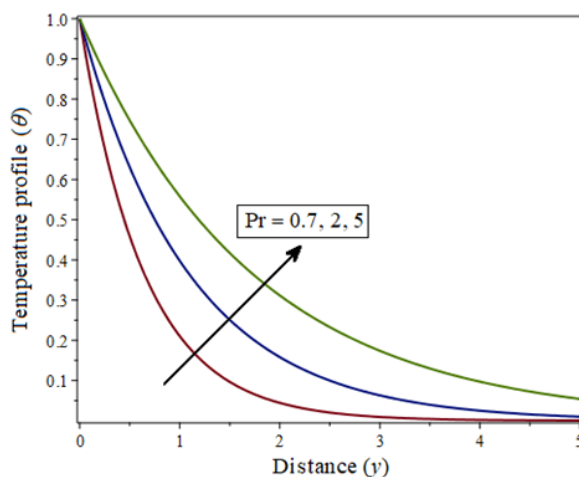


Figure 9. An illustration profile of Temperature for various values of Pr.

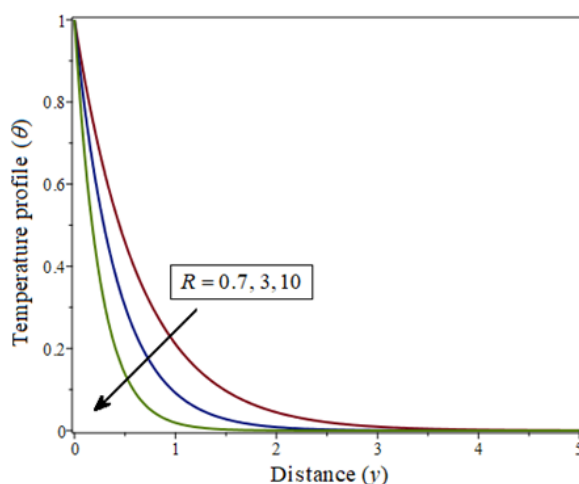


Figure 10. An illustration profile of Temperature for various values of R.

The influence of Pr, R, γ , Sc, and Sr on the concentration profiles ϕ is shown in Figures 11–15. The fluid concentration rises on highest values of Pr, as shown in Figure 11. The profile of temperature is affected by the radiation parameter R which is shown in Figure 12. As a function of R, the concentration profiles reduce the flow and decrease fluid velocity.

The growing values of γ and Sc lead to falling in the concentration profiles, is described from Figures 13 and 15. The concentration profiles increase as the number of sorts (Sr) increases, as shown in Figure 14.

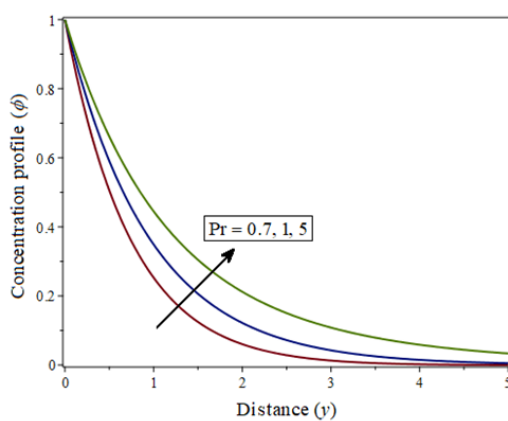


Figure 11. Profile of concentration for distinct values of Pr.

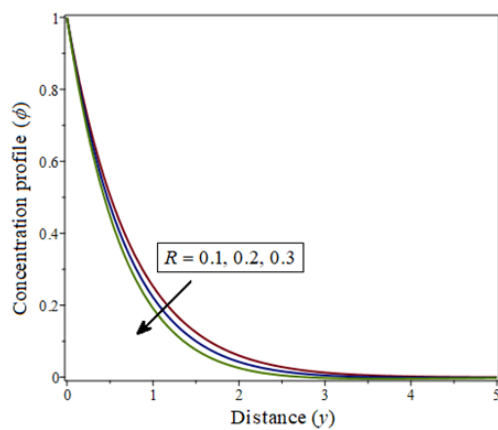


Figure 12. Profile of concentration for distinct values of R.

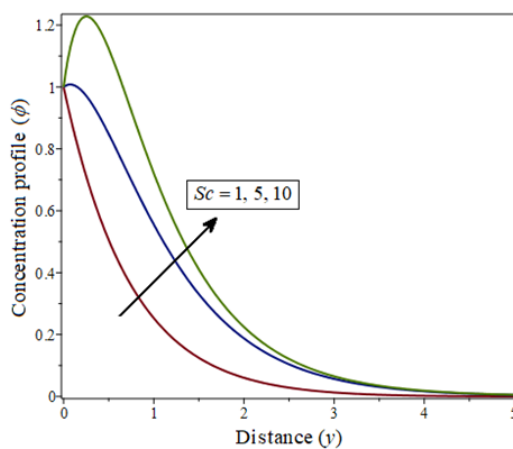


Figure 13. Profile of concentration for distinct values of Sc.

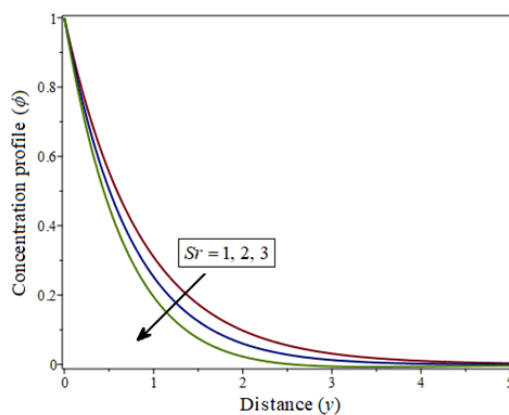


Figure 14. Profile of concentration for distinct values of Sr .

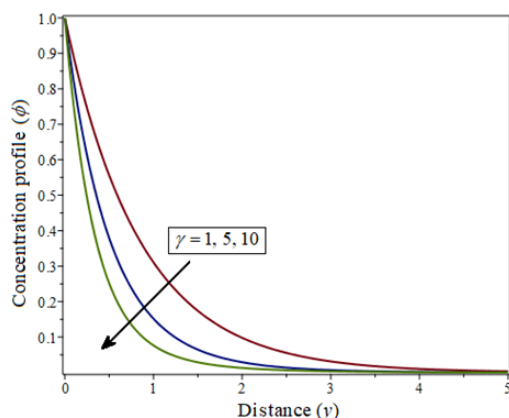


Figure 15. Profile of concentration for distinct values of γ .

6. Conclusions

A free convection magnetohydrodynamic (MHD) flow past a vertical plate embedded in a porous medium was offered in this paper. Homotopy perturbation method is used to find approximate analytical solutions for the concentration of species. The effects of system parameters on temperature and velocity profiles were investigated using these analytical expressions. The graphic representation of the impact of several physical parameters attempting to control the velocity, temperature, and concentration profiles and a brief discussion. Analytical expressions were also developed for the Skin-friction and Nusselt and Sherwood numbers.

Conflict of interest

The authors declare that they have no conflict of interest.

Acknowledgement

The authors are thankful to the reviewers for their valuable comments and suggestions to improve the quality of the paper. The work of H. Alotaibi is supported by Taif University Researchers Supporting Project Number (TURSP-2020/304), Taif University, Taif, Saudi Arabia.

References

1. M. Garnier, Magneto hydrodynamics in materials processing, *Philos. Trans. R. Soc. Phys. Sci. Eng.*, **344** (1962), 249–263.
2. A. Chakrabarti, A. S. Gupta, Hydromagnetic flow and heat transfer over a stretching sheet, *Quart Appl. Math.*, **37** (1979), 13–78. <https://doi.org/10.1090/qam/99636>
3. S. Nadeem, U. I. HaqRizwana, C. Lee, MHD flow of a casson fluid over an exponentially shrinking sheet, *Sci. Iran.*, **19** (2012), 1550–1553. <https://doi.org/10.1016/j.scient.2012.10.021>
4. K. Bhattacharya, MHD stagnation point flow of casson fluid and heat transfer over a stretching sheet with thermal radiation, *J. Thermody.*, **2013** (2013), Article ID 169674. <https://doi.org/10.1155/2013/169674>
5. A. Ishak, R. Nazar, I. Pop, Mixed convection on the stagnation pit flow toward a vertical, continuously stretching sheet, *J. Heat Transfer*, **129** (2007), 1087–1090. <https://doi.org/10.1115/1.2737482>
6. A. Ishak, R. Nazar, I. Pop, Post stagnation point boundary layer flow and mixed convection heat transfer over a vertical, linearly stretching sheet, *Arch. Mech.*, **60** (2008), 303–322.
7. A. Ishak, K. Jafar, R. Nazar, Pop, MHD stagnation point flow towards a stretching sheet, *Physics A*, **388** (2009), 3377–3383. <https://doi.org/10.1016/j.physa.2009.05.026>
8. S. Gala, M. A. Ragusa, Y. Sawano, H. Tanaka, Uniqueness criterion of weak solutions for the dissipative quasi-geostrophic equations in Orlicz–Morrey spaces, *Appl. Anal.*, **93** (2014), 356–368. <https://doi.org/10.1080/00036811.2013.772582>
9. R. P. Agarwal, O. Bazighifan, M. A. Ragusa, Nonlinear neutral delay differential equations of fourth-Order: Oscillation of solutions, *Entropy*, **23** (2021), 129. <https://doi.org/10.3390/e23020129>
10. T. Hayat, M. Bilal Ashraf, S. A. Shehzad, A. Alsaedi, Mixed convection flow of Cassonnanofluid over a stretching sheet with convectively heated chemical reaction and heat source/sink, *J. Appl. Fluid Mech.*, **8** (2015), 803–813. <https://doi.org/10.18869/acadpub.jafm.67.223.22995>
11. M. S. Abel, M. Mareppa, MHD flow and heat transfer of the mixed hydrodynamic/thermal slip over a linear vertically stretching sheet, *Int. J. Math. Archive*, **4** (2013), 156–163.
12. M. Shen, F. Wang, H. Chen, MHD mixed convection slip flow near a stagnation point on a non-linearly vertical stretching sheet, *Boundary Value Probl.*, **2015** (2015), 78. <https://doi.org/10.1186/s13661-015-0340-6>
13. N. Ashikin, A. Bakar, W. MohdKhairy, A. W. Zaimi, R. A. Hamid, B. Bidin, et al., Boundary layer flow over a stretching sheet with a convective boundary condition and slip effect, *World Appl. Sci. J.*, **17** (2012), 49–53.

14. M. A. Imran, S. Sarwar, M. Imran, Effects of slip on free convection flow of Casson fluid over an oscillating vertical plate, *Boundary Value Probl.*, **2016** (2016), 30. <https://doi.org/10.1186/s13661-016-0538-2>
15. N. Uddin Md, A. MA, MMK. Chowdhury, Effects of mass transfer on MHD mixed convective flow along inclined porous plate, *Procedia Eng.*, **90** (2014), 491–496. <https://doi.org/10.1016/j.proeng.2014.11.762>
16. R. N. Barik, G. C. Dash, Thermal radiation effect on an unsteady magnetohydrodynamic flow past inclined porous heated plate in the presence of chemical reaction and viscous dissipation, *Appl. Math. Comput.*, **226** (2014), 423–434. <https://doi.org/10.1016/j.amc.2013.09.077>
17. R. M. Ramana, J. G. Kumar, Chemical reaction effects on MHD free convective flow past an inclined plate, *Asian J. Current Eng. Math.*, **3** (2014), 66–71.
18. H. Mondal, D. Pal, S. Chatterjee, P. Sibanda, Thermophoresis and Soret-Dufour on MHD mixed convection mass transfer over an inclined plate with non-uniform heat source/sink and chemical reaction, *Ain Shams Eng. J.*, **9** (2018), 2111–2121. <https://doi.org/10.1016/j.asej.2016.10.015>
19. F. Ali, I. Khan, S. Shafie, N. Musthapa, Heat and mass transfer with free convection MHD flow past a vertical plate embedded in a porous medium, *Math. Probl. Eng.*, **2013** (2013), Art. ID 346281, 13 pp. <https://doi.org/10.1155/2013/346281>
20. S. Thamizh, P. Suganya, L. Balaganesan, M. A. Rajendran, Analytical discussion and sensitivity analysis of parameters of magnetohydrodynamic free convective flow in an inclined plate, *Eur. J. Pure Appl. Math.*, **13** (2020), 631–644. <https://doi.org/10.29020/nybg.ejpm.v13i3.3730>
21. H. He, Homotopy perturbation technique, *Comput. Methods Appl. Mech. Eng.*, **178** (1999), 257–262. [https://doi.org/10.1016/S0045-7825\(99\)00018-3](https://doi.org/10.1016/S0045-7825(99)00018-3)
22. J. H. He, Application of homotopy perturbation method to non-linear wave equations, *Chaos Soliton. Fract.*, **26** (2005), 695–700. <https://doi.org/10.1016/j.chaos.2005.03.006>
23. A. Meena, L. Rajendran, Mathematical modeling of amperometric and potentiometric biosensors and system of non-linear equations Homotopy perturbation approach, *J. Electroanal. Chem.*, **644** (2010), 50–59. <https://doi.org/10.1016/j.jelechem.2010.03.027>
24. S. T. Suganya, P. Balaganesan, J. Visuvasam, L. Rajendran, An analytical expression of Non-Nernstian catalytic mechanism at Micro and Macro electrodes at voltammetry, *Asia Matematika*, **5** (2021), 1–10.



AIMS Press

© 2022 the Author(s), licensee AIMS Press. This is an open access article distributed under the terms of the Creative Commons Attribution License (<http://creativecommons.org/licenses/by/4.0>)